Pullout Strength of Suture Anchors Used in Rotator Cuff Repair

Markus J. Tingart, Maria Apreleva, David Zurakowski and Jon J.P. Warner
J Bone Joint Surg Am. 85:2190-2198, 2003.

Pullout Strength of Suture Anchors Used in Rotator Cuff Repair

By Markus J. Tingart, MD, Maria Apreleva, PhD, David Zurakowski, PhD, and Jon J.P. Warner, MD

Investigation performed at the Orthopaedic Biomechanics Laboratory, Beth Israel Deaconess Medical Center, Department of Orthopaedic Surgery, Massachusetts General Hospital, Harvard Medical School, Boston, Massachusetts

Background: Surgical treatment of rotator cuff tears may be complicated by osteoporosis of the proximal part of the humerus. The purpose of this study was to determine whether pullout strength of suture anchors is affected by the location of the anchor placement and by bone mineral density. We hypothesized that higher bone mineral density is associated with higher pullout strength of suture anchors.

Methods: Peripheral quantitative computed tomography was used to measure total, trabecular, and cortical bone mineral density in different regions of the lesser and greater tuberosities in seventeen cadaveric humeri. Suture anchors were inserted into individual regions and subjected to cyclic loading. Repeated-measures analysis of variance was used to assess differences in bone mineral density and load to failure between regions of interest. Pearson correlation was used to determine the association between bone mineral density and pullout strength of suture anchors.

Results: Total, trabecular, and cortical bone mineral densities were an average of 50%, 50%, and 10% higher, respectively, in the proximal part of the tuberosities compared with the distal part ($p < 0.01$). Within the proximal part of the greater tuberosity, trabecular bone mineral density of the posterior region and cortical bone mineral density of the middle region were, on the average, 25% and 16% higher, respectively, than the densities in the other regions ($p < 0.01$). Load to failure in the proximal part of the tuberosities was an average of 53% higher than that in the distal part ($p < 0.01$). The lesser tuberosity showed, on the average, a 32% higher load to failure than did the greater tuberosity ($p < 0.01$). Within the proximal part of the greater tuberosity, loads to failure in the anterior and middle regions were, on the average, 62% higher than the load to failure in the posterior region ($p < 0.01$). Overall positive correlations were found between bone mineral density and load to failure ($0.65 \leq r \leq 0.74$, $p < 0.01$).

Conclusions: We found that pullout strength of suture anchors correlates well with bone mineral density of the tuberosities. Higher loads to failure were found in regions in the proximal part of the tuberosities. Placement of anchors in these regions may prevent anchor loosening, formation of a tendon-bone gap, and failure of the rotator cuff repair.

Rotator cuff tears are common injuries in patients over sixty years of age[1]. These patients can also have osteoporosis of the proximal part of the humerus, which can be aggravated by chronic progression of a rotator cuff tear[2-6].

Three major factors determine the success of a rotator cuff repair: suture material, tendon-grasping technique, and tendon-to-bone fixation[5,7]. With advances in arthroscopic surgery, the use of suture anchors has become more popular because of the ease and speed of their use and because of the decreased surgical exposure and morbidity[8-10].

Rotator cuff repairs with suture anchors and transosseous sutures were found to have high fixation strength in experimental studies[5,7,10-13]. However, the applicability of these findings might be limited since most of the studies were performed in porcine specimens, which are not representative of human bones. Furthermore, we are not aware of any studies that have accounted for bone density changes in elderly patients. In such patients, the strength of rotator cuff repairs might be compromised by a decrease in bone quality, resulting in suture anchors pulling out of bone and transosseous sutures cutting through bone before the tendon heals[5,7,14,15]. In biomechanical studies performed on human humeri, rotator cuff repairs frequently have failed at the bone interface[9,14,16,17]. Djurasovic et al. reported, in a clinical study, that eight of eighty patients needed surgical revision of a rotator cuff repair because of migration and loosening of suture anchors[18].

Barber et al.[7] and Goradia et al.[19] attempted to correlate the bone quality of the humeral head with the pullout strength of suture anchors. Those investigators used two-dimensional dual-energy x-ray absorptiometry to study the bone mineral density of the proximal part of the humerus. Barber et al. found pullout strength in the anterior part of the greater tu-

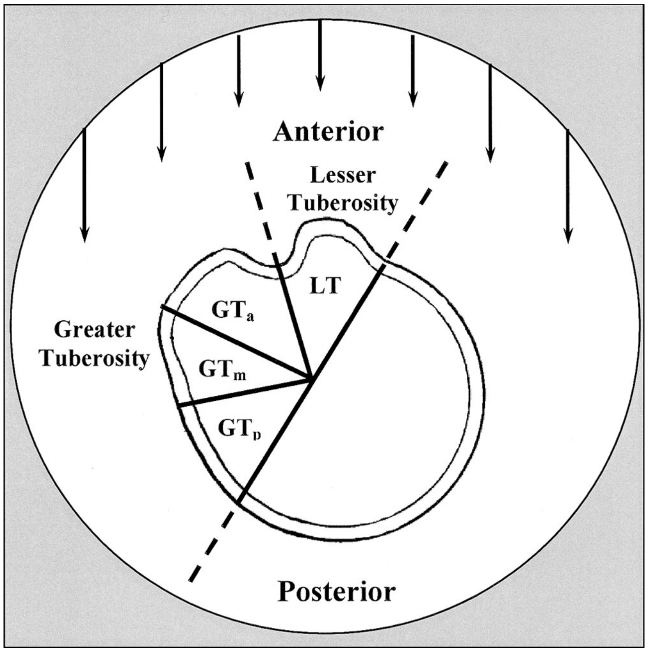

Fig. 1

The proximal part of the humerus was horizontally fixed with the lesser tuberosity in the twelve o'clock position for assessment of bone mineral density. The regions of interest were defined as the lesser tuberosity (LT), the anterior region of the greater tuberosity (GT_a), the middle region of the greater tuberosity (GT_m), and the posterior region of the greater tuberosity (GT_p). The arrows indicate the direction of the scanning beam of the peripheral quantitative computed tomography.

berosity (96 N) to be 40% lower than that in the posterior part (160 N). Neither study showed a significant difference in total bone mineral density among the various regions of the greater tuberosity, and no correlation was seen between pullout strength of suture anchors and total bone mineral density. The two-dimensional dual-energy x-ray absorptiometry technique used in those studies allowed measurement of only total bone mineral density; it was not possible to discriminate between trabecular and cortical bone mineral density[7,19].

Current anchor designs may vary with regard to the type of bone on which they rely for fixation. For example, hook-like anchors may rely more on a strong cortical layer of the humeral head, whereas the pullout strength of screw-like anchors may be affected by both trabecular and cortical bone[7]. Therefore, a more systematic analysis of three-dimensional bone mineral density and its cortical and trabecular distribution may be needed to identify a potential association between the bone mineral density of the humeral head and the pullout strength of suture anchors. The purpose of this study was to quantitatively assess total, trabecular, and cortical bone mineral density of clinically relevant regions within the greater and lesser tuberosities and to determine whether there was a relationship between pullout strength, the location of anchor placement, and bone mineral density.

We hypothesized that higher bone mineral density of the humeral head region was associated with higher pullout strength of suture anchors.

Materials and Methods

Preparation of Specimens

Twenty unpaired fresh-frozen human humeri were harvested and were stored at –20°C. The specimens were thawed at room temperature for twenty-four hours before testing. After thawing, they were dissected and all soft tissue was removed. All specimens had a macroscopically intact rotator cuff. Biplanar radiographs were used to identify bone abnormalities. Specimens with a previous proximal humeral fracture, underlying pathologic changes, or evidence of surgical intervention were excluded. Three specimens were excluded on the basis of these criteria, and seventeen specimens (twelve from male donors and five from female donors, with a mean age of seventy years [range, fifty-nine to ninety-eight years] at the time of death) were included in the study.

Bone Mineral Density of the Greater and Lesser Tuberosities

The total, trabecular, and cortical bone mineral density of the greater and lesser tuberosities was measured with use of peripheral quantitative computed tomography (XCT-960A; Norland/Stratec, Fort Atkinson, Wisconsin)[20,21]. For these measurements, each humerus was fixed horizontally in a custom-made jig with the lesser tuberosity in the twelve o'clock position (Fig. 1). Axial scans of each specimen were made to determine bone mineral density (pixel size, 0.59 mm; slice thickness, 2.5 mm; slice separation, 2 mm). The inferior border of the humeral head was determined by a horizontal line running through the lowest point of the articular surface. All computed tomography scans were performed and analyzed by the same investigator.

On the cross-sectional view, four specific regions of interest were determined on the middle computed tomography image of the humeral head. A diagonal line separated the articular surface from the tuberosities, and a second line, running though the center of the bicipital groove, separated the

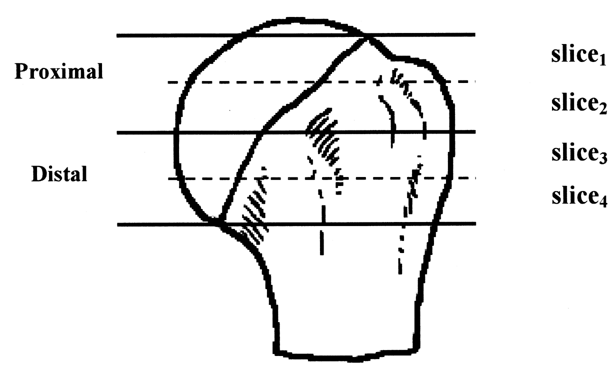

Fig. 2

The humeral head was divided into four levels ($slice_1$ through $slice_4$). The proximal part of the head comprises $slice_1$ and $slice_2$, and the distal part of the head comprises $slice_3$ and $slice_4$.

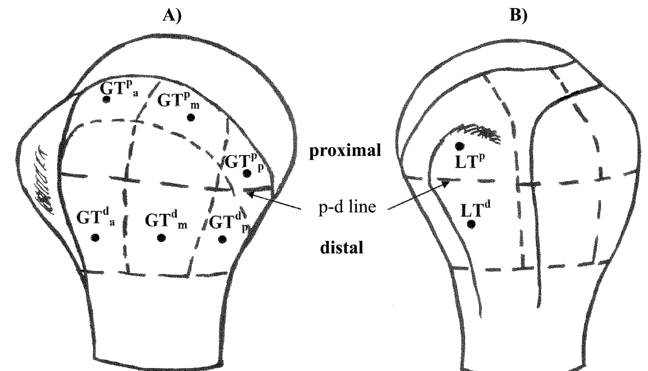

Fig. 3

Locations of anchor placement in the proximal and distal parts of the greater and lesser tuberosities. Proximal anchors were inserted in the middle between the border of the articular surface and the tip of the greater or lesser tuberosity. Distal anchors were inserted in the center of the distal part of each region of interest. The p-d (proximal-distal) line separates the proximal and distal halves of the humeral head. The locations of anchor placement in the greater tuberosity *(A)* include the proximal anterior region (GTP^p_a), proximal middle region (GT^p_m), proximal posterior region (GTP^p_p), distal anterior region (GT^d_a), distal middle region (GT^d_m), and distal posterior region (GT^d_p). The locations of anchor placement in the lesser tuberosity *(B)* are the proximal region (LT^p) and the distal region (LT^d).

lesser from the greater tuberosity (Fig. 1). The greater tuberosity was divided into three regions of interest: anterior (GT_a), middle (GT_m), and posterior (GT_p) (Fig. 1). These regions of interest were copied automatically to each image of the same specimen. An average of nineteen images was made for each specimen, with a range of sixteen to twenty-three images, depending on the size of the humeral head.

The humeral head was divided into four slices of the same height, which were designated, from proximal to distal, as $slice_1$ through $slice_4$ (Fig. 2). The total and trabecular areas of the anterior, middle, and posterior regions of the greater tuberosity and of the lesser tuberosity were contoured manually on the middle computed tomography image of $slice_1$ through $slice_4$. When the total area was contoured for the anterior region of the greater tuberosity and for the lesser tuberosity, the cortical bone of the bicipital grove was excluded because suture anchors are not usually inserted in that location. All contouring was performed by the same investigator, who following a standardized pre-hoc protocol. The coefficient of variation for determining the bone mineral density of the specific regions of interest was <3% (0.7% for total bone mineral density, 0.8% for trabecular bone mineral density, and 2.7% for cortical bone mineral density). Automatic determination of these parameters was not possible as the software was not capable of distinguishing between cortical and trabecular bone in regions that were not completely surrounded by cortical bone. Total and trabecular bone mineral density and bone mineral content were determined separately for the proximal ($slice_1$ + $slice_2$) and distal ($slice_3$ + $slice_4$) parts of each region of interest. The cortical bone mineral density was calculated on the basis of the difference between the total and trabecular volumes and the difference between the total and trabecular bone mineral contents.

Pullout Tests of Suture Anchors

Following peripheral quantitative computed tomography scanning, each proximal humeral specimen was potted in polymethylmethacrylate approximately 10 mm below the distal border of the humeral head. To ensure that our manually defined regions of interest on each humeral head were identical to the corresponding regions of interest on the peripheral quantitative computed tomography scans, we followed a strict, standardized protocol. The inferior border of the humeral head was defined as the lowest point of the articular surface and was marked with a horizontal line on each specimen (Fig. 3). The border between the proximal and distal parts of the humeral head was determined with digital calipers (Mitutoyo, Tokyo, Japan; measurement error, ±0.02 mm) and marked with a horizontal line (proximal-distal line). A vertical line running through the interface of the proximal-distal line with the anterior border of the articular surface marked the anterior border of the lesser tuberosity, and a vertical line running through the interface of the proximal-distal line and the posterior border of the articular surface determined the posterior border of the greater tuberosity. A line running through the deepest point of the bicipital groove on the proximal-distal line separated the greater from the lesser tuberosity. With use of a tape measure with 1-mm subdivisions, the greater tuberosity was divided into six regions: proximal anterior (GT^p_a), proximal middle (GT^p_m), proximal posterior (GT^p_p), distal anterior (GT^d_a), distal middle (GT^d_m), and distal posterior (GT^d_p) (Fig. 3, *A*). The lesser tuberosity was divided, in the same manner, into two regions: proximal (LT^p) and distal (LT^d) (Fig. 3, *B*).

Metal screw-like suture anchors (5-mm Fastin RC; Mitek, Norwood, Massachusetts) were placed in the proximal and distal parts of each region of interest. Proximal anchors were placed in the middle between the articular surface and the tip of

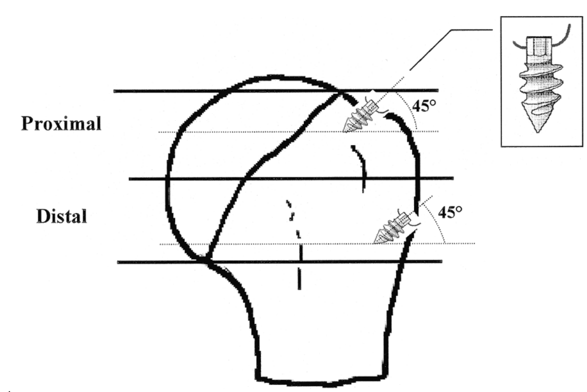

Fig. 4

A cross-sectional diagram in the coronal plane showing the insertion angle of the suture anchors with respect to the articular margin and the cortex of the humerus in the proximal and distal parts of the humeral head, respectively.

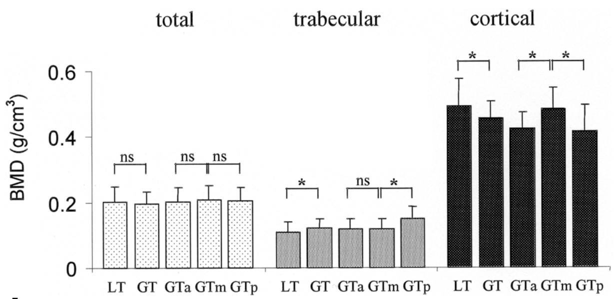

Fig. 5

Total, trabecular, and cortical bone mineral density (BMD) (mean and standard deviation) of different regions of interest in the proximal part of the humeral head. LT = lesser tuberosity, GT = greater tuberosity, GTa = anterior part of the greater tuberosity, GTm = middle part of the greater tuberosity, and GTp = posterior part of the greater tuberosity. *$p < 0.01$.

the greater or lesser tuberosity. Distal anchors were inserted 10 to 15 mm distal to the tip of the greater or lesser tuberosity, in the center of the distal part of each region of interest. Anchors were inserted at a 45° angle to the bone surface (Fig. 4)[22]. We used self-tapping metal screw-like anchors. According to the manufacturer's recommendations, the anchors were inserted into the bone without predrilling a pilot hole. To exclude any interference when the pullout testing was performed, the distance between the sites of anchor insertion was at least 10 mm, as recommended previously[17,23]. Since we were investigating the relationship between pullout strength of suture anchors and bone quality, the original sutures were replaced by 0.62-mm-diameter steel wire (McMaster-Carr Supply, Chicago, Illinois) to eliminate suture breakage as a mode of failure[10]. The proximal part of the humerus was then fixed in a customized jig. The steel wire was secured in a handmade clamp, with a distance of 40 mm between the tip of the anchor and the clamp. The clamp was connected to a materials testing machine (Bionix 200; MTS Systems, Eden Prairie, Minnesota), and the humeral head was oriented in such a way that load was applied parallel to the axis of anchor insertion[10]. This testing setup was previously established in a number of studies by Barber et al., and it simulates the worst-case scenario for failure strength of suture anchors[10-12].

Anchors were cyclically loaded with a preload of 4 N and an extension rate of 1 mm/sec. A 50-N maximum load was chosen for the first ten cycles, and this was increased in 50-N increments after each ten cycles. A maximum of forty cycles was performed (maximum load, 200 N). Linear load to failure was then applied to the anchors that had not pulled out after forty cycles. For each pullout test, the load to failure, number of cycles completed, and stiffness of the anchor fixation were determined. Real-time data acquisition was performed with use of TestWorks (version 4.04 B; MTS Systems). Load-elongation data for each anchor in each region of interest were recorded. Stiffness was calculated for cycles ten, twenty, thirty, and forty according to the slope of the load-elongation curve between the 10% and 90% points of the maximum load.

Statistical Analysis

A power analysis indicated that a sample size of seventeen specimens would provide statistical power of 86% to detect mean differences in load to failure of one standard deviation between the regions of interests of the lesser and greater tuberosities ($\beta = 0.1$, $\alpha = 0.01$). The Kolmogorov-Smirnov test was used to evaluate whether load to failure and bone mineral density followed a normal (gaussian-shaped) distribution, and no significant departures were identified[24]. Repeated-measures analysis of variance was used to compare load to failure and bone mineral density between regions of interest. The stiffnesses of the anchor fixation were compared between the proximal and distal parts of the tuberosities with use of paired t tests. A two-tailed t test ($p < 0.01$) was chosen a priori to declare a significant result, to account for multiple comparisons[25,26]. The Pearson product-moment correlation coefficient (r) was calculated to evaluate the linear association between bone mineral density and load to failure. Stepwise multiple linear regression analysis was used to determine whether cortical and trabecular bone mineral density were significant predictors of load to failure and number of completed cycles with respect to each region of interest within the proximal and distal parts of the humeral head[24]. Prediction equations were derived on the basis of the significant variables in the final stepwise models. Data analysis was performed with use of the SPSS statistical package (version 11.0; SPSS, Chicago, Illinois). Power calculations were determined with use of the nQuery Advisor software package (version 4.0; Statistical Solutions, Boston, Massachusetts). Continuous data are presented as means and standard deviations.

Results

Differences in Bone Mineral Density Between the Proximal and Distal Regions of Interest

The proximal part of the tuberosities had higher total, trabecular, and cortical bone mineral densities than the distal part ($p < 0.01$) (Figs. 5 and 6; Table I). Within the lesser tuberosity, total and trabecular bone mineral densities were higher in the proximal part than they were in the distal part

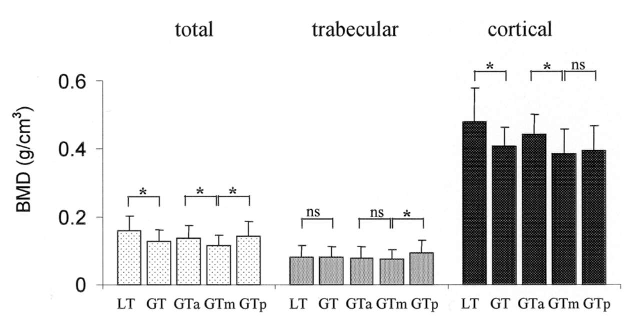

Fig. 6

Total, trabecular, and cortical bone mineral density (BMD) (mean and standard deviation) of different regions of interest in the distal part of the humeral head. LT = lesser tuberosity, GT = greater tuberosity, GTa = anterior part of the greater tuberosity, GTm = middle part of the greater tuberosity, and GTp = posterior part of the greater tuberosity. *$p < 0.01$.

TABLE I Differences in Bone Mineral Density Between Proximal and Distal Parts According to Regions of Interest*

Region of Interest	Proximal†	Distal†	Mean Difference (Proximal – Distal)†	P Value‡
Total bone mineral density *(g/cm³)*				
Tuberosities	0.21 ± 0.04	0.14 ± 0.03	0.07 ± 0.02	<0.01
LT	0.20 ± 0.05	0.16 ± 0.04	0.04 ± 0.03	<0.01
GT	0.20 ± 0.04	0.13 ± 0.03	0.07 ± 0.02	<0.01
GT_a	0.20 ± 0.05	0.14 ± 0.04	0.06 ± 0.03	<0.01
GT_m	0.21 ± 0.04	0.11 ± 0.03	0.10 ± 0.02	<0.01
GT_p	0.20 ± 0.04	0.14 ± 0.04	0.06 ± 0.04	<0.01
Trabecular bone mineral density *(g/cm³)*				
Tuberosities	0.12 ± 0.03	0.08 ± 0.03	0.04 ± 0.01	<0.01
LT	0.11 ± 0.03	0.08 ± 0.03	0.03 ± 0.02	<0.01
GT	0.12 ± 0.03	0.08 ± 0.03	0.04 ± 0.02	<0.01
GT_a	0.12 ± 0.03	0.08 ± 0.03	0.04 ± 0.02	<0.01
GT_m	0.12 ± 0.03	0.07 ± 0.03	0.05 ± 0.02	<0.01
GT_p	0.15 ± 0.04	0.09 ± 0.04	0.06 ± 0.03	<0.01
Cortical bone mineral density *(g/cm³)*				
Tuberosities	0.46 ± 0.06	0.42 ± 0.06	0.04 ± 0.04	<0.01
LT	0.49 ± 0.09	0.48 ± 0.10	0.01 ± 0.07	NS
GT	0.45 ± 0.05	0.41 ± 0.06	0.04 ± 0.04	<0.01
GT_a	0.42 ± 0.05	0.44 ± 0.06	–0.02 ± 0.05	NS
GT_m	0.48 ± 0.06	0.38 ± 0.07	0.10 ± 0.06	<0.01
GT_p	0.41 ± 0.08	0.39 ± 0.07	0.02 ± 0.08	NS

*LT = lesser tuberosity; GT = greater tuberosity; and GT_a, GT_m, and GT_p = anterior, middle, and posterior regions, respectively, of the greater tuberosity. See Figures 1 and 3 for the specific locations of the anchor insertions. †Data are given as the mean and standard deviation. ‡A p value of <0.01 indicates a significant difference between the proximal and distal parts. All p values were determined by repeated-measures analysis of variance with seventeen specimens for each comparison. NS = not significant.

($p < 0.01$), but there was no significant difference between the proximal and distal regions with regard to cortical bone mineral density ($p = 0.70$). In addition, the proximal part of the greater tuberosity showed higher total, trabecular, and cortical bone mineral densities than did the distal part ($p < 0.01$). All regions of interest (anterior, middle, and posterior) in the greater tuberosity showed higher total and trabecular bone mineral densities in the proximal part than in the distal part, whereas cortical bone mineral density was higher in the proximal part than in the distal part only in the middle region of the greater tuberosity ($p < 0.01$).

Differences in Trabecular and Cortical Bone Mineral Densities Between Regions of Interest

The proximal part of the greater tuberosity showed a higher trabecular and a lower cortical bone mineral density than did the proximal part of the lesser tuberosity ($p < 0.01$) (Fig. 5). No difference in trabecular bone mineral density was found between the distal parts of the greater and lesser tuberosities ($p = 0.71$), but cortical bone mineral density was higher in the distal part of the lesser tuberosity than in the distal part of the greater tuberosity ($p < 0.01$) (Fig. 6). Within the proximal part of the greater tuberosity, trabecular bone mineral density was higher in the posterior region than in the anterior region or the middle region ($p < 0.01$). Within the distal part of the greater tuberosity, trabecular bone mineral density was higher in the posterior region than in the middle region ($p < 0.01$). Furthermore, within the proximal part of the greater tuberosity, cortical bone mineral density was higher in the middle region than in the posterior region or the anterior region ($p < 0.01$). Finally, within the distal part of the greater tuberosity, cortical bone mineral density was higher in the anterior region than in the posterior or middle region ($p < 0.01$).

Pullout Strength of Suture Anchors in Specific Regions of Interest

The proximal part of the tuberosities demonstrated a higher load to failure and number of cycles than did the distal part ($p < 0.01$) (Table II). In addition, in both the lesser and the greater tuberosity, the load to failure and the number of cycles were higher in the proximal part than in the distal part ($p < 0.01$). Within the greater tuberosity, load to failure was higher in the proximal middle region and proximal anterior region compared with their respective distal parts ($p < 0.01$), whereas no significant difference was detected between the proximal posterior and distal posterior regions.

Anchors inserted into the proximal and distal parts of the lesser tuberosity showed higher loads to failure than those placed in the greater tuberosity ($p < 0.01$) (Table II). Within the proximal part of the greater tuberosity, load to failure was higher in the anterior and middle regions than it was in the posterior region ($p < 0.01$). Within the distal part of the greater tuberosity, no significant differences in load to failure were seen among the anterior, middle, and posterior regions.

Stiffness of the Anchor Fixation

The stiffnesses of the anchor fixation did not differ significantly between the proximal and distal parts of the tuberosities at 50 N (44 ± 5 N/mm compared with 45 ± 6 N/mm, respectively), 100 N (94 ± 8 N/mm compared with 92 ± 9 N/mm), 150 N (137 ± 9 N/mm compared with 130 ± 12 N/mm), or 200 N (166 ± 15 N/mm compared with 158 ± 12 N/mm) (all $p > 0.10$, paired t tests). At 200 N, the stiffness value was based on only eight specimens, since the majority of the anchors failed at lower loads. In addition, no differences in stiffness were found between the greater and lesser tuberosities or between any other regions of interest.

Correlation Between Bone Mineral Density and Pullout Strength

There was a significant correlation between each of the bone mineral density parameters (total, trabecular, and cortical) and load to failure. The highest correlation was between total bone mineral density and load to failure (correlation coefficient: $r = 0.74$, $p < 0.01$), but trabecular bone mineral density (correlation coefficient: $r = 0.71$, $p < 0.01$) and cortical bone mineral density (correlation coefficient: $r = 0.65$, $p < 0.01$) also had a significant positive correlation with load to failure.

Regression Modeling of Loads to Failure

In the proximal part of the greater tuberosity, cortical bone mineral density was a significant multivariate predictor of load to failure in the greater tuberosity ($t = 2.84$, $p = 0.012$), in the anterior region of the greater tuberosity ($t = 2.63$, $p = 0.018$), and in the posterior region of the greater tuberosity ($t = 4.16$, $p < 0.001$ for cortical and trabecular bone mineral density). In the distal part of the greater tuberosity, trabecular bone mineral density was a significant multivariate predictor of load to failure in the greater tuberosity ($t = 3.08$, $p = 0.008$) and the posterior ($t = 2.63$, $p = 0.019$), middle ($t = 3.53$, $p = 0.003$), and anterior ($t = 2.75$, $p = 0.015$) regions of the greater tuberosity.

In the proximal part of the lesser tuberosity, trabecular bone mineral density was a significant multivariate predictor of load to failure ($t = 4.76$, $p < 0.001$). In the distal part of the lesser tuberosity, cortical bone mineral density was a significant multivariate predictor of load to failure ($t = 2.43$, $p = 0.028$).

Table III shows fitted regression models for prediction of load to failure by cortical and trabecular bone mineral density in each region of interest.

TABLE II Differences in Load to Failure and Number of Cycles Between Proximal and Distal Parts According to Regions of Interest*

Region of Interest	Proximal†	Distal†	Mean Difference (Proximal – Distal)†	P Value‡
Failure load *(N)*				
Tuberosities	290 ± 110	189 ± 55	101 ± 80	<0.01
LT	333 ± 155	209 ± 73	124 ± 143	<0.01
GT	244 ± 95	169 ± 54	75 ± 65	<0.01
GT_a	275 ± 136	164 ± 57	111 ± 106	<0.01
GT_m	284 ± 144	165 ± 67	119 ± 140	<0.01
GT_p	173 ± 68	179 ± 66	–6 ± 67	NS
No. of cycles				
Tuberosities	32 ± 6	27 ± 7	5 ± 5	<0.01
LT	36 ± 8	29 ± 9	6 ± 9	<0.01
GT	30 ± 7	25 ± 9	5 ± 6	<0.01
GT_a	31 ± 11	24 ± 9	7 ± 8	<0.01
GT_m	32 ± 10	25 ± 10	7 ± 14	NS
GT_p	26 ± 11	26 ± 11	0 ± 10	NS

*LT = lesser tuberosity; GT = greater tuberosity; and GT_a, GT_m, and GT_p = anterior, middle, and posterior regions, respectively, of the greater tuberosity. See Figures 1 and 3 for the specific locations of the anchor insertions. †Data are given as the mean and standard deviation. ‡A p value of <0.01 indicates a significant difference between the proximal and distal parts. All p values were determined by repeated-measures analysis of variance with seventeen specimens for each comparison. NS = not significant.

TABLE III Fitted Regression Models for Cortical and Trabecular Bone Mineral Density in Predicting Loads to Failure*

Region of Interest	Fitted Regression Equation for Load to Failure Prediction	R^2 Value
Proximal part		
LT	y = 3885.7 × trabecular bone mineral density – 86.5	0.68
GT	y = 1117.6 × cortical bone mineral density – 253.7	0.40
GT_p	y = 538.0 × cortical bone mineral density + 718.2 × trabecular bone mineral density – 157.0	0.73
GT_m	No fitted regression model was derived	
GT_a	y = 1498.5 × cortical bone mineral density – 358.9	0.38
Distal part		
LT	y = 959.3 × cortical bone mineral density – 137.6	0.29
GT	y = 1013.1 × trabecular bone mineral density – 86.2	0.43
GT_p	y = 1037.0 × trabecular bone mineral density + 81.7	0.37
GT_m	y = 1541.7 × trabecular bone mineral density + 50.5	0.50
GT_a	y = 1018.3 × trabecular bone mineral density + 83.6	0.40

*LT = lesser tuberosity; GT = greater tuberosity; and GT_a, GT_m, and GT_p = anterior, middle, and posterior regions, respectively, of the greater tuberosity. See Figures 1 and 3 for the specific locations of the anchor insertions.

Discussion

Poor fixation of suture anchors due to reduced bone quality of the proximal part of the humerus is a major problem in rotator cuff repair[4,5,7,9,14,17,18]. Pullout of suture anchors before tendon-healing may result in gap formation between the tendon and the bone, rupture of the rotator cuff repair, and a poor outcome[4,5,7,14,19]. Recommendations in the literature regarding the optimum region for placement of suture anchors in rotator cuff repair are controversial[8,13,19,27,28]. Surgeons are limited to the region of the greater and lesser tuberosity when reattaching the torn rotator cuff. The site of tendon reattachment is influenced by the size of the rotator cuff tear, the involved rotator cuff tendons, the degree of tendon retraction, and the amount of tendon mobilization achieved as well as the degree of tendon tension during the rotator cuff surgery[8,27,28]. However, within these limitations, the surgeon still has some options regarding where to reaffix the torn rotator cuff. In an experimental study, Rossouw et al. found that suture anchors placed 25 mm distal of the tip of the greater tuberosity had higher pullout strengths[13]. The authors speculated that a higher cortical thickness might be the reason for this increase in pullout strength and therefore recommended insertion of anchors as far distal from the tip of the greater tuberosity as possible. Furthermore, some review articles have recommended placing suture anchors lateral and distal to the greater tuberosity because the bone stock was thought to be better in that area[8,27]. In contrast, in other studies, a position medial to the tip of the tuberosities was thought to be favorable for insertion of suture anchors[19,28].

Previous pullout tests of suture anchors in human proximal humeral specimens showed the loads to failure to be only between 90 and 180 N[5,7]. We found higher loads to failure, averaging 240 N and ranging from 173 to 333 N, depending on the bone site where the anchors had been inserted. The higher pullout forces in our study might be attributed to differences in anchor design and the way in which loads were applied. Load to failure was determined with cyclic testing rather than linear pullout because cyclic testing is a more physiologic approach of assessing loads applied to the rotator cuff following repair[9,28].

We found a significant correlation between bone mineral density and the pullout strength of suture anchors. Regression modeling of load to failure showed cortical bone mineral density to be a better predictor of pullout strength in the proximal part of the greater tuberosity than trabecular bone mineral density, whereas trabecular bone mineral density was a better predictor of load to failure in the distal part of the greater tuberosity. When only total bone mineral density is analyzed, the correlation between bone mineral density and pullout strength is not that obvious because total bone mineral density is a combination of trabecular and cortical bone mineral density. This would explain the findings of Barber et al.[7] and Goradia et al.[19], who investigated the correlation between total bone mineral density and pullout strength and found no correlation between them.

We investigated the effect of bone mineral density on the pullout strength of a metal screw-like suture anchor. However, other anchors that differ in material, size, and design are currently available for rotator cuff repair, and they may have shown different failure patterns and loads to failure[7,19]. Also, the association between bone mineral density and the pullout strength of other anchor types, such as hook-like suture anchors, might differ from the correlations found in our study. We chose the metal screw-like anchor because it is one of the most commonly used anchors.

In the past, creation of a cancellous trough during rotator cuff repair was recommended to improve tendon-to-bone healing[29]. However, in 1995, St. Pierre et al. demonstrated, in a biomechanical and histological study, that there is no significant benefit to creating this trough to expose tendon to cancellous bone[30]. Shoulder surgeons use different methods to attach the rotator cuff to bone. When performing arthroscopic repairs, most surgeons abrade the bone surface at the attachment site for the rotator cuff, rather than removing the cortical bone and creating a trough in the cancellous bone[7,9,19,23,27,31]. Therefore, in our experimental model, cortical bone was not removed and no cancellous trough was created before anchor placement.

In addition to bone mineral density, other parameters such as trabecular microarchitecture of bone may affect the pullout strength of suture anchors[7]. Insertion of anchors at a 45° angle to the bone surface is recommended in clinical situations, as this is perpendicular to the direction of rotator cuff pull[22]. Therefore, we inserted the anchors at a 45° angle in our experimental model, to ensure the same trabecular alignment as is present in clinical situations. However, the direction of pull during testing was parallel to the axis of the suture anchor, since this simulates the worst-case scenario of failure strength. These testing conditions were previously established and justified by a number of studies by Barber et al., who investigated the bone-anchor interface[7,10-12]. Nevertheless, one might speculate that pullout strength is higher when anchors are tested perpendicular to the insertion angle, especially when the anchors were inserted distal to the tip of the greater or lesser tuberosity, but this scenario was not evaluated in our model. In our study, all of the anchors failed by pulling out of the bone; we did not observe any bone fractures or wire breakage. This mechanism of failure might differ from that observed on testing of whole rotator cuff repair constructs or when biodegradable anchors are used. The mode of failure in those situations could include anchor-eyelet cutout, suture breakage, or tendon slipping[9,10,19]. Since the main goal of this project was to investigate the relationship between bone mineral density and anchor pullout strength, simulation of other failure modes was beyond the scope of the study.

In conclusion, we recommend insertion of suture anchors medial to the tip of the greater tuberosity and particularly in the proximal-anterior and proximal-middle regions, which provide the best bone stock. We cannot confirm the previous suggestions that there is better cortical bone stock and higher anchor pullout strength distal to the tip of the greater tuberosity. Placement of anchors in the regions that we recommended would provide stronger fixation within the tuberosities and may prevent anchor loosening, formation of a tendon-bone gap, and failure of the rotator cuff repair. ■

NOTE: The authors acknowledge the continuous assistance of Dr. Bouxsein throughout this study.

Markus J. Tingart, MD
Maria Apreleva, PhD
Orthopaedic Biomechanics Laboratory, Beth Israel Deaconess Medical Center, Harvard Medical School, 330 Brookline Avenue, RN 115, Boston, MA 02215. E-mail address for M. Apreleva: maria.apreleva@gmx.net

David Zurakowski, PhD
Departments of Orthopaedic Surgery and Biostatistics, Children's Hospital, 300 Longwood Avenue, Boston, MA 02115

Jon J.P. Warner, MD
Department of Orthopaedic Surgery, Massachusetts General Hospital, 275 Cambridge Street, Suite 403, Boston, MA 02114

In support of their research or preparation of this manuscript, one or more of the authors received grants or outside funding from Deutsche Forschungsgemeinschaft, Orthopaedic Research Laboratories Alumni Council. None of the authors received payments or other benefits or a commitment or agreement to provide such benefits from a commercial entity. No commercial entity paid or directed, or agreed to pay or direct, any benefits to any research fund, foundation, educational institution, or other charitable or nonprofit organization with which the authors are affiliated or associated. Mitek Products (Ethicon, Johnson and Johnson) donated the suture anchors.

References

1. **Sher JS, Uribe JW, Posada A, Murphy BJ, Zlatkin MB.** Abnormal findings on magnetic resonance images of asymptomatic shoulders. *J Bone Joint Surg Am.* 1995;77:10-5.
2. **Rose SH, Melton LJ 3rd, Morrey BF, Ilstrup DM, Riggs BL.** Epidemiologic features of humeral fractures. *Clin Orthop.* 1982;168:24-30.
3. **Bengner U, Johnell O, Redlund-Johnell I.** Changes in the incidence of fracture of the upper end of the humerus during a 30-year period. A study of 2125 fractures. *Clin Orthop.* 1988;231:179-82.
4. **Gerber C, Fuchs B, Hodler J.** The results of repair of massive tears of the rotator cuff. *J Bone Joint Surg Am.* 2000;82:505-15.
5. **Gerber C, Schneeberger AG, Beck M, Schlegel U.** Mechanical strength of repairs of the rotator cuff. *J Bone Joint Surg Br.* 1994;76:371-80.
6. **Kannus P, Leppala J, Lehto M, Sievanen H, Heinonen A, Jarvinen M.** A rotator cuff rupture produces permanent osteoporosis in the affected extremity, but not in those with whom shoulder function has returned to normal. *J Bone Miner Res.* 1995;10:1263-71.
7. **Barber FA, Feder SM, Burkhart SS, Ahrens J.** The relationship of suture anchor failure and bone density to proximal humerus location: a cadaveric study. *Arthroscopy.* 1997;13:340-5.
8. **Gartsman GM.** Arthroscopic rotator cuff repair. *Clin Orthop.* 2001;390:95-106.
9. **Craft DV, Moseley JB, Cawley PW, Noble PC.** Fixation strength of rotator cuff repairs with suture anchors and the transosseous suture technique. *J Shoulder Elbow Surg.* 1996;5:32-40.
10. **Barber FA, Herbert MA.** Suture anchors—update 1999. *Arthroscopy.* 1999;15:719-25.
11. **Barber FA, Herbert MA, Click JN.** Suture anchor strength revisited. *Arthroscopy.* 1996;12:32-8.
12. **Barber FA, Herbert MA, Click JN.** Internal fixation strength of suture anchors—update 1997. *Arthroscopy.* 1997;13:355-62.
13. **Rossouw DJ, McElroy BJ, Amis AA, Emery RJ.** A biomechanical evaluation of suture anchors in repair of the rotator cuff. *J Bone Joint Surg Br.* 1997;79:458-61.
14. **Hecker AT, Shea M, Hayhurst JO, Myers ER, Meeks LW, Hayes WC.** Pull-out strength of suture anchors for rotator cuff and Bankart lesion repairs. *Am J Sports Med.* 1993;21:874-9.
15. **Harryman DT 2nd, Mack LA, Wang KY, Jackins SE, Richardson ML, Matsen FA 3rd.** Repairs of the rotator cuff. Correlation of functional results with integrity of the cuff. *J Bone Joint Surg Am.* 1991;73:982-9.
16. **Sward L, Hughes JS, Amis A, Wallace WA.** The strength of surgical repairs of the rotator cuff. A biomechanical study on cadavers. *J Bone Joint Surg Br.* 1992;74:585-8.
17. **Reed SC, Glossop N, Ogilvie-Harris DJ.** Full-thickness rotator cuff tears. A biomechanical comparison of suture versus bone anchor techniques. *Am J Sports Med.* 1996;24:46-8.

18. **Djurasovic M, Marra G, Arroyo JS, Pollock RG, Flatow EL, Bigliani LU.** Revision rotator cuff repair: factors influencing results. *J Bone Joint Surg Am.* 2001;83:1849-55.

19. **Goradia VK, Mullen DJ, Boucher HR, Parks BG, O'Donnell JB.** Cyclic loading of rotator cuff repairs: a comparison of bioabsorbable tacks with metal suture anchors and transosseous sutures. *Arthroscopy.* 2001;17:360-4.

20. **Genant HK, Engelke K, Fuerst T, Gluer CC, Grampp S, Harris ST, Jergas M, Lang T, Lu Y, Majumdar S, Mathur A, Takada M.** Noninvasive assessment of bone mineral and structure: state of the art. *J Bone Miner Res.* 1996; 11:707-30.

21. **Mirsky EC, Einhorn TA.** Bone densitometry in orthopaedic practice. *J Bone Joint Surg Am.* 1998;80:1687-98.

22. **Burkhart SS.** The deadman theory of suture anchors: observations along a south Texas fence line. *Arthroscopy.* 1995;11:119-23.

23. **Schneeberger AG, von Roll A, Kalberer F, Jacob HA, Gerber C.** Mechanical strength of arthroscopic rotator cuff repair techniques: an in vitro study. *J Bone Joint Surg Am.* 2002;84:2152-60.

24. **Sokal RR, Rohlf FJ.** *Biometry: the principles and practice of statistics in biological research.* 3rd ed. New York: WH Freeman; 1995.

25. **Altman DG, Gore SM, Gardner MJ, Pocock SJ.** Statistical guidelines for contributors to medical journals. *Br Med J (Clin Res Ed).* 1983;286:1489-93.

26. **Lang TA, Secic M.** *How to report statistics in medicine: annotated guidelines for authors, editors, and reviewers.* Philadelphia: American College of Physicians; 1997. p 81-92.

27. **Ticker JB, Warner JJ.** Single-tendon tears of the rotator cuff. Evaluation and treatment of subscapularis tears and principles of treatment for supraspinatus tears. *Orthop Clin North Am.* 1997;28:99-116.

28. **Burkhart SS, Diaz Pagan JL, Wirth MA, Athanasiou KA.** Cyclic loading of anchor-based rotator cuff repairs: confirmation of the tension overload phenomenon and comparison of suture anchor fixation with transosseous fixation. *Arthroscopy.* 1997;13:720-4.

29. **Crenshaw AH, editor.** Shoulder and elbow injuries. In: *Campbell's operative orthopaedics.* 8th ed. St. Louis: Mosby-Year Book; 1992. p 1745.

30. **St. Pierre P, Olson EJ, Elliott JJ, O'Hair KC, McKinney LA, Ryan J.** Tendon-healing to cortical bone compared with healing to a cancellous trough. A biomechanical and histological evaluation in goats. *J Bone Joint Surg Am.* 1995;77:1858-66.

31. **Burkhart SS, Fischer SP, Nottage WM, Esch JC, Barber FA, Doctor D, Ferrier J.** Tissue fixation security in transosseous rotator cuff repairs: a mechanical comparison of simple versus mattress sutures. *Arthroscopy.* 1996;12:704-8.